J Nanopart Res (2026) 28:56
https://doi.org/10.1007/s11051-026-06581-6

RESEARCH

$CuSn(OH)_6$ nanoparticles as a novel adsorbent for the preconcentration of cadmium ions in onion extract

Meltem Şaylan · Selim Gürsoy · Ümmügülsüm Polat Korkunç · Buse Tuğba Zaman · Sezgin Bakırdere

Received: 29 November 2025 / Accepted: 9 February 2026

Abstract The present study aims to develop a new preconcentration strategy for the determination of non-essential cadmium ions in red onion samples. Determination of the extracted cadmium ions was carried out using flame atomic absorption spectrometry for efficient and sensitive detection. The synthesis of $CuSn(OH)_6$ nanoparticles was accomplished via a single-step one-pot coprecipitation method under ambient conditions to obtain nanoparticles below 100 nm in size, which are particularly effective for preconcentration procedures. The morphology and structure of the nanoparticles were confirmed with different characterization techniques. Under the optimized conditions, the calibration curve of the presented method showed good linearity between 2.5 and 50 µg/L, with a detection limit of 0.84 µg/L. The accuracy of this method was confirmed by obtaining recoveries of spiked red onion extracts. This method offers a sensitive, efficient, and eco-friendly method for the separation/detection of trace cadmium ions in aqueous plant-derived matrixes, especially red onion extracts.

Keywords Cadmium · $CuSn(OH)_6$ nanoparticles · Preconcentration · Flame atomic absorption spectrometry · Onion

M. Şaylan · Ü. P. Korkunç · B. T. Zaman · S. Bakırdere (✉)
Department of Chemistry, Yıldız Technical University, 34220 Istanbul, Türkiye
e-mail: bsezgin23@yahoo.com

M. Şaylan
Department of Pharmacy, İstanbul Health and Technology University, 34421 Istanbul, Türkiye

S. Gürsoy
Department of Analytical Chemistry, School of Pharmacy, İstanbul Medipol University, 34810 Istanbul, Türkiye

S. Gürsoy
Department of Bioengineering, Yıldız Technical University, 34220 Istanbul, Türkiye

S. Bakırdere
Turkish Academy of Sciences (TÜBA), Vedat Dalokay Street, No: 112, 06670, Çankaya, Ankara 06690, Türkiye

Introduction

The onion is a biennial plant belonging to the Alliaceae family [7, 16]. Onions are among the most consumed vegetables in the world due to their characteristic aroma and taste, high content of health-beneficial components, and good storability. From a medical perspective, it has been widely used to treat many diseases including asthma, atherosclerosis, diabetes, high blood pressure, and various cardiovascular and tumor diseases [6]. Red onions, a variety of *Allium cepa*, have a white interior with red stripes and a purplish-red exterior [27]. Pharmacological and biological studies have revealed that bioactive compounds obtained from onions have potential antioxidant functions and are effective in preventing cardiovascular

Published online: 17 February 2026

and neurological diseases. In addition, these bioactive compounds exhibit anticarcinogenic activity, antidiabetic potential, antimicrobial activity, and antimutagenic activity [14]. The majority of the known active ingredients of onion consist of two major groups of compounds, including sulfur compounds and flavonoids [13]. The polyphenol quercetin is one of the main plant-derived flavonoids that is abundant in onion peels [19]. Soil is vital for the nutrition of all food crops, and the soil has been significantly polluted by heavy metals emitted from both point and non-point sources in recent years. Thus, beneficial soil insects in soil biota, invertebrates, and small and large mammals have been adversely affected by heavy metals. Heavy metals are easily absorbed by plant species through the root system and can significantly accumulate in their edible parts [5].

The heavy metals are defined by metallic properties and associated with pollution and biological toxicity for living beings. Cadmium is classified as a "non-essential" heavy metal, which has no biological function [26]. There is a proven link between food cross-contamination by heavy metals, environmental pollution, and the food chain, and this issue emerges as a nutritional hazard. Accordingly, serious systemic health problems can develop because of contamination of basic dietary components such as onions, carrots, and potatoes and the accumulation of excessive amounts of dietary heavy metals in the human body [40]. In humans, Ca is responsible for regulating normal heart rhythms, helping muscles contract, bone and teeth health, and nerve functions, while Cd substitutes Ca and translocates due to similar properties such as equal charges and comparable ionic radii. Therefore, the World Health Organization (WHO) has established a monthly consumption limit of Cd ions of 25 µg/kg body weight, and Cd content is limited to 3.0 µg/L in drinking water (Y. [21, 22]). The presence of toxic heavy elements, including Al, Cd, Hg, Pb, etc., can display a health risk depending on their oxidation states at high concentrations in medicinal herbs and their mixtures for human beings [2]. For example, the presence of toxic metals causes serious health issues such as dysfunction of the central nervous system, brain, heart, liver, kidneys, and lungs [1].

Inductively coupled plasma mass spectrometry (ICP-MS) [29], inductively coupled plasma optical emission spectrometry (ICP-OES) [36], and flame atomic absorption spectrometry (FAAS) [1] are widely applied spectroscopic techniques for elemental analysis of plant samples. FAAS is a commonly employed spectroscopic method due to its affordability and ease of use, while the determination of trace levels of Cd in natural samples is affected by low analyte concentration and matrix effects. Overcoming these challenges requires preconcentration and matrix elimination steps [8]. Advanced sample preparation methods increasingly focus on "greener" approaches, such as reducing sample and solvent consumption, generating low-cost sorbents for cleanup and analytical processes, and equipment miniaturization [31]. Despite this trend, many conventional preconcentration strategies used for Cd and other heavy metals still rely on liquid-liquid extraction and co-precipitation, which can provide high enrichment factors but usually require large volumes of organic solvents, multiple handling steps, and relatively long extraction times [37, 43]. In contrast, solid-phase extraction (SPE) and solid-phase microextraction (SPME) rely on small amounts of sorbent and sample, offer easier automation and coupling to FAAS, and better comply with green analytical chemistry principles. Thus, SPME approaches that deploy the sorbent directly in the sample solution require high-surface-area, water-compatible materials capable of rapid metal uptake, making the choice of sorbent a critical factor in the overall preconcentration performance [32].

Metal hexahydroxystannates ($MSn(OH)_6$; M = Co, Cu, Zn, etc.) are a type of transition metal stannate that possess excellent physical and chemical properties due to their unique crystal structure, and offer a variety of sizes, shapes, and morphologies. $MSn(OH)_6$ offers intrinsic advantages, including large specific surface area, low cost, eco-friendly, morphological diversity, and high catalytic activity [34]. Their high surface area, abundance of surface hydroxyl groups, and ion-exchange capability make $MSn(OH)_6$ type materials attractive sorbents for solid-phase extraction and microextraction-based preconcentration of metal ions (Z. [23]). Several studies have been reported for the synthesis of $MSn(OH)_6$, involving co-precipitation, hydrothermal methods, and sonochemical methods [11]. The perovskite-structured metal hexahydroxystannate $CuSn(OH)_6$, which exhibits ReO_3 lattice connectivity, has received significant attention due to its large specific surface area with eco-friendliness and affordability (J.

[21, 22]). Herein, $CuSn(OH)_6$ nanoparticles have been successfully synthesized via a simple one-pot coprecipitation method and used as adsorbent material for the preconcentration of Cd ions.

In the present study, the main objective was to develop a new $CuSn(OH)_6$ nanoparticle-assisted preconcentration strategy for the determination and monitoring of Cd ions in onion extracts using flame atomic absorption spectrometry (FAAS). $CuSn(OH)_6$ nanoparticles were synthesized by a simple coprecipitation procedure performed at ambient temperature (~25℃), providing an operationally straightforward and time-efficient route to the sorbent material. Owing to their facile preparation and favorable surface properties, $CuSn(OH)_6$ nanoparticles represent promising sorbents for the monitoring of environmental contamination and heavy metal pollution.

Materials and methods

Chemicals and reagents

The Cd(II) stock solution (1.0 g/L in 0.5 M HNO_3) was purchased from Merck (Germany) and used for the preparation of serial dilutions of standard/working solutions. Deionized water produced by the Elga Pure Flex 3 Ultrapure Water system (18.2 Ω cm resistivity, UK) served for sample preparation and cleaning. $CuSn(OH)_6$ nanoparticles were synthesized using $CuCl_2$ and anhydrous $SnCl_4$ supplied by Merck (Germany), and sodium citrate and NaOH were sourced from Isolab (Germany). The concentrated HNO_3 solution (65%, w/w) was used as a desorption solution supplied by Merck (Germany) and systematically diluted with deionized water to prepare the desired concentration. The buffer solution (pH 8.0) was prepared with borax and HCl solution, which was purchased from Merck, Germany. The other chemicals required for the preparation of the buffer solution were purchased from Merck (Germany) with analytical-reagent grade. Acetylene gas with purity grade 2.0 was supplied from HABAŞ (Turkey) and used for the fuel of the FAAS system. Onion samples used in recovery studies were purchased from the local greengrocer in İstanbul, Turkey.

Instrumentation

All absorbance measurements were performed by an atomic absorption spectrometer equipped with a flame burner and deuterium background corrector (ATI UNICAM 929 AA system, Cambridge, UK). A Cd multi-hollow cathode lamp (Photron Lamp, Australia) was used, operating with a maximal current of 10 mA, a bandpass of 0.5 nm, and a wavelength of 228.8 nm, and other operating conditions were set to the manufacturer's instructions. The digital pH meter (Hanna Multiparameter, HI2020) was used for the pH measurement and adjustment. The weighing of materials was done using an OHAUS Pioneer PA214C model analytical balance with a sensitivity of 0.1 mg. A BIOBASE brand (BKC-TL5II model) centrifuge was employed to separate the nanoparticles from the aqueous phase. The stirring process was accomplished by the ultrasonic water bath (Hapa M-100 model), orbital shaker (BIOBASE brand SK-O330-Pro model), and vortex (Isolab, Germany). The X-ray diffraction (XRD) analysis was conducted with the Bruker D2 PHASER model (Germany), and morphology analysis was acquired with the scanning electron microscope (SEM) (Zeiss EVO LS 10 model, Jena, Germany). Fourier Transform Infrared Spectroscopy (FT-IR) (Perkin ELMER Spectrum Two) was used to determine the structural analysis of the synthesized nanomaterials.

Synthesis of CuSn(OH)6 nanoparticles

$CuSn(OH)_6$ nanoparticles were prepared by modifying previously reported procedures [24, 44]. $CuSn(OH)_6$ nanoparticles were prepared via a facile co-precipitation method at room temperature. The synthesis procedure is briefly as follows: $CuCl_2$ (0.0218 mol) and sodium citrate (0.0218 mol) were dissolved in 200 mL of deionized water in the 500-mL flask. Subsequently, 2.56 mL of anhydrous $SnCl_4$ solution (0.0218 mol) was added to this solution at ambient conditions with continuous stirring. 100 mL of 2.0 M NaOH solution was introduced dropwise into the reaction medium. Upon completion of a one-hour reaction period, the blue-greenish precipitate was collected by centrifugation and thoroughly rinsed with deionized water followed by ethanol in cycles to eliminate excessive chemicals and unreacted materials. The rinsed materials underwent overnight drying

in an oven at 50–55 °C and were crushed in a porcelain mortar. The crushed materials were characterized by XRD, SEM, and FT-IR. The synthesized material was preserved in a polypropylene tube and stored in a wooden cabinet at room temperature before the analysis.

Experimental procedure

Thirty milliliters of standard/test solution was added to the 50 mL polypropylene test tubes containing 40 mg of $CuSn(OH)_6$ nanoparticles. 2.0 mL of pH 8.0 borax buffer solution was used for the adjustment of the test solutions. The uniform distribution of nanoparticles was achieved by ultrasonic bath for 30 s. The nanoparticles were then separated with the help of centrifugation for 2.0 min (3000 rpm). After the centrifugation process, the clear upper aqueous phase was carefully disposed of using a pipette into the disposal. One hundred eighty microliters of 4.0 M nitric acid solution was added into the collected samples, and desorption was completed by vortexing for 15 s. Following this process, the samples were centrifuged again at 3000 rpm (2.0 min), and $CuSn(OH)_6$ nanoparticles were easily separated. The analyte-rich acidic homogeneous phase was pipetted to a clean tube without touching the bottom of the tube. The analyte-rich acid phase was directly sent to the FAAS system without any filtration. Figure 1 indicates the experimental procedures of the optimized method.

Sampling and preparation of extracts

Red onions (RO) were purchased in the spring of 2025 from different local greengrocers in İstanbul, Turkey. Sample preparation steps are briefly as follows: The fresh red onions were conventionally peeled to remove outer layers and cut into small pieces using a plastic knife to avoid potential metal contamination. Considering traditional consumption, the fresh samples were directly used without the drying process to preserve the natural moisture content and water-soluble components. 50 g of RO samples were then weighed and transferred into a 500 mL Erlenmeyer flask. Two hundred milliliters of the boiling deionized water (95–100 °C) was added to the onion samples, followed by cooling to ambient temperature. The resulting aqueous onion extract was subsequently diluted tenfold with deionized water used in the specified procedure. The same sample pretreatment process was applied for samples and spiked samples. The onion samples obtained from two different sources were coded as RO-1 and RO-2, respectively.

Results and discussion

Characterization studies

The FT-IR spectrum of the synthesized $CuSn(OH)_6$ nanoparticles was recorded within the region of

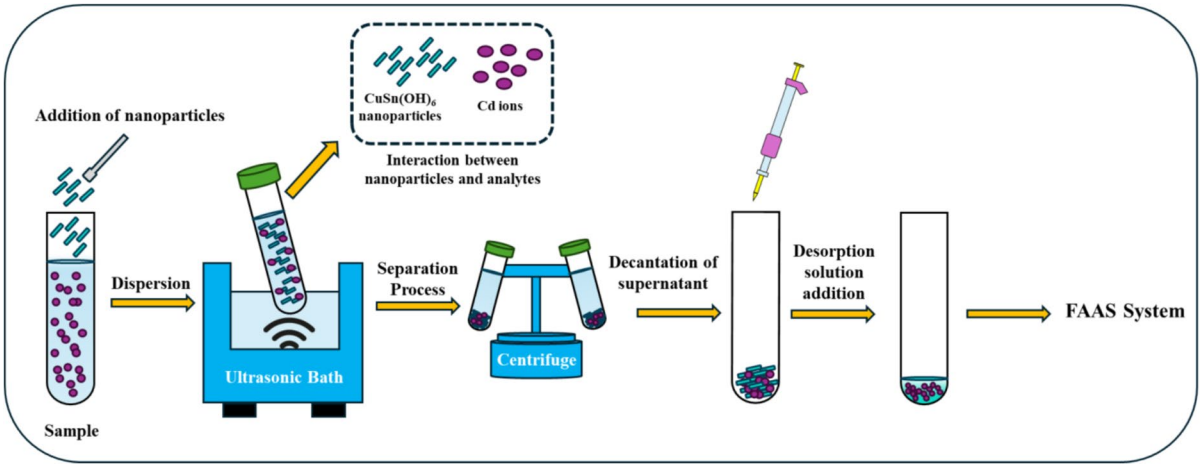

Fig. 1 Scheme of preconcentration process under optimized conditions

400–4000 cm^{-1}, and the distinctive vibrational bands verify the formation of a hydrated $CuSn(OH)_6$ structure (Fig. 2). A broad and sharp absorption band apparent at 3571 cm^{-1} and 3294 cm^{-1} is ascribed to the stretching vibrations of hydrogen-bonded -OH groups from lattice-bound or adsorbed water molecules. These peaks indicate the presence of structural hydroxyl groups, an essential characteristic of $CuSn(OH)_6$. The peaks at 1378 cm^{-1}, 1157 cm^{-1}, and 936 cm^{-1} correspond to δ(OH) bending vibrations and/or coordinated water molecules in the hydroxide structure. The prominent peaks at 694 cm^{-1} and 519 cm^{-1} correspond to metal-O stretching vibrations associated with Cu–O and Sn–O bonds. The peak at 416.44 cm^{-1} indicates the infrared-active modes for $Cu(OH)_2$. These align with the vibrational modes reported for musinonite-type $CuSn(OH)_6$ and analogous mixed hydroxides [10, 28, 33].

The crystalline structure of the synthesized $CuSn(OH)_6$ nanoparticles was examined using X-ray diffraction (XRD) in the 2θ range of 10°—90°, with Cu Kα radiation (λ = 1.5406 Å). The diffractogram exhibits sharp and peaks at approximately 2θ = 19.8°, 21.9°, 23.4°, 32.3°, 33,40°, 40,3°, 51.0°, and 59.0°, which are characteristic of $CuSn(OH)_6$ (PDF# 04-017-7356, musinonite), confirming the formation of a crystalline mixed copper-tin hydroxide phase. Minor additional reflections matched with $Cu(OH)_2$ (PDF# 04-009-4366, spertiniite) indicate a small amount of secondary phase, likely due to incomplete incorporation of copper during synthesis (Fig. 3). The broadness of the peaks suggests nanocrystalline size, and no peaks corresponding to tin oxides were detected, indicating high phase selectivity [17, 28].

Scanning electron microscope (SEM) images evidenced the formation of well-defined nanoparticles with a highly uniform size distribution below 100 nm. As seen in Fig. 4, the $CuSn(OH)_6$ nanoparticles exhibit a remarkably uniform morphology with minimal agglomeration, indicating successful synthesis conditions.

Optimization of preconcentration conditions for Cd extraction and desorption

The various parameters impacting extraction and desorption conditions were assessed to achieve a high enrichment factor/extraction efficiency with

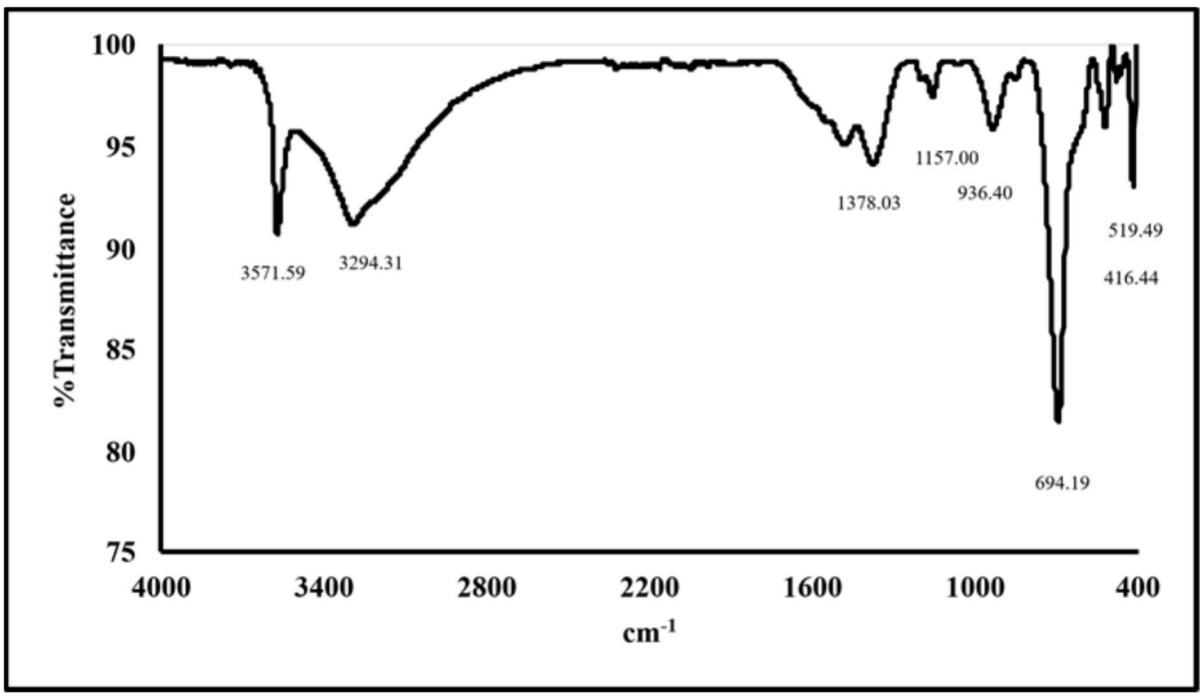

Fig. 2 The FT-IR spectrum of $CuSn(OH)_6$ nanoparticles

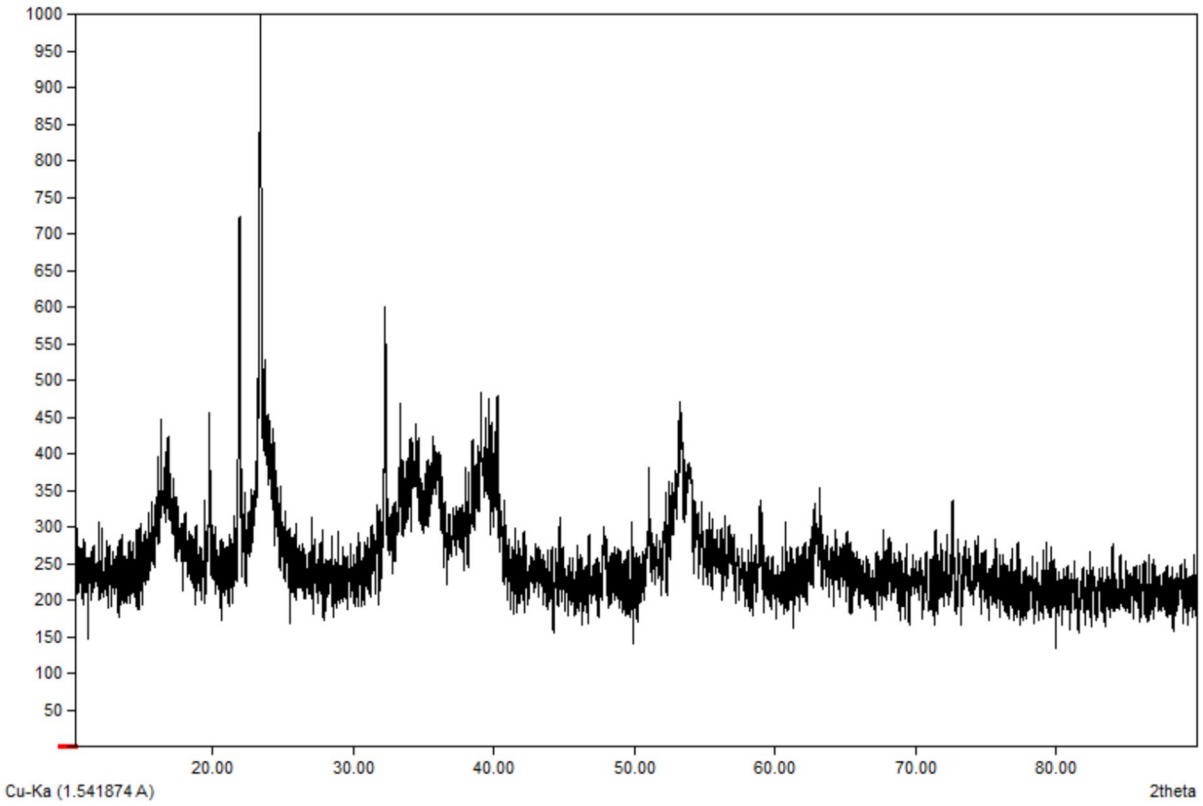

Fig. 3 The XRD patterns for $CuSn(OH)_6$ nanoparticles

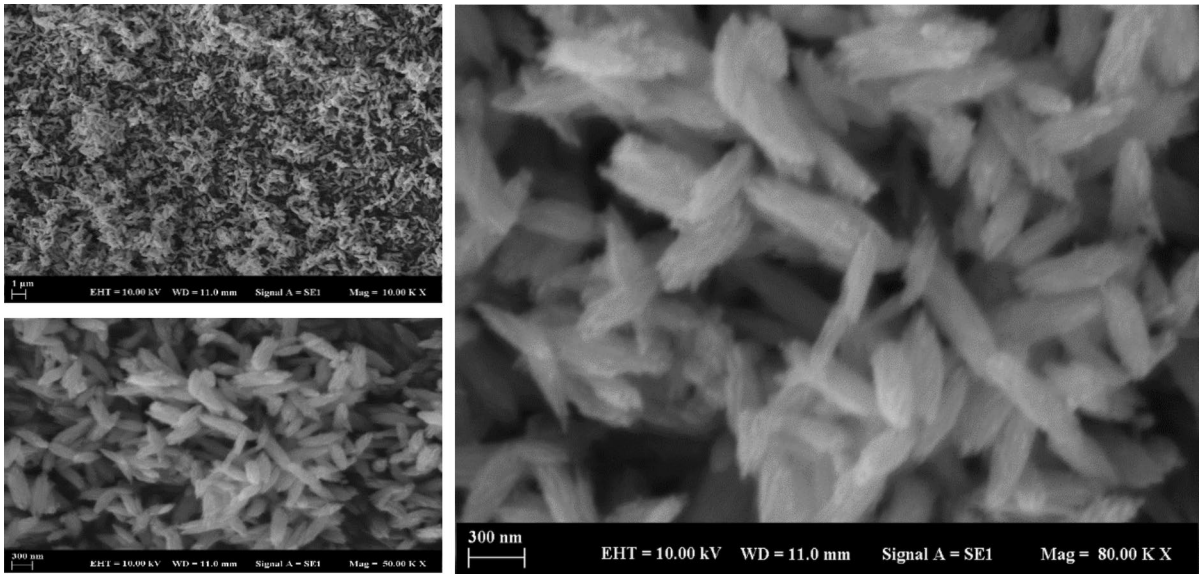

Fig. 4 SEM images of the CuSn(OH) nanoparticles

the recommended preconcentration method. The variables were examined using a univariate optimization approach, in which one parameter was changed while the others remained constant. Each optimization factor was conducted in replicate experiments ($n = 3$) to ensure analytical precision and data reliability. The optimal conditions were selected using absorbance values and standard deviation (*SD*) of replicate measurements. Statistical analysis of the collected data was made with the assistance of Microsoft Excel software (Microsoft Inc., USA) to calculate basic statistical parameters, comprehensive analysis, and graphical representation of findings. Initial sample volume was maintained constant at 30 mL during all optimization experiments to facilitate and accelerate the extraction/desorption step. The optimized conditions are listed in Table 1.

Effect of sample pH

To obtain maximum recovery of analyte in the preconcentration process, adjusting the pH of the sample solution is an important requirement. This is because pH affects the surface charge distribution and thus determines the stability of the nanomaterial [4]. Additionally, the pH of the aqueous samples impacts the performance of the adsorption process due to the metal ions with negative or positive charges [30]. The suggested method was performed within a pH range of 4.0–8.0 to establish the optimal pH level (Fig. 5a). Firstly, 20 mg of sorbent was dispersed in 30 mL test solution and 4.0 mL of different buffer solution. The samples were mixed with the help of the orbital shaker for 15 min. Then, the samples were centrifugated and approximately 2.0 mL of the upper phase was sent to the FAAS system. The quantitative recovery values were obtained at pH 6.0–8.0, whereas low removal efficiencies were obtained at lower pH < 6.0. At lower pH values, removal efficiency is estimated

Table 1 Optimal conditions of the presented method

Variable	Optimal condition
Working/sample solution volume	**30 mL**
Buffer solution pH/volume	**pH 8.0 borax buffer solution/2.0 mL**
Nanomaterial amount	**40 mg $CuSn(OH)_6$ nanoparticles**
Mixing type/period	**Ultrasonication/30 s**
Desorption solution conc./volume	**4.0 M HNO_3/0.180 mL**
Mixing period after the desorption	**15 s vortexing**

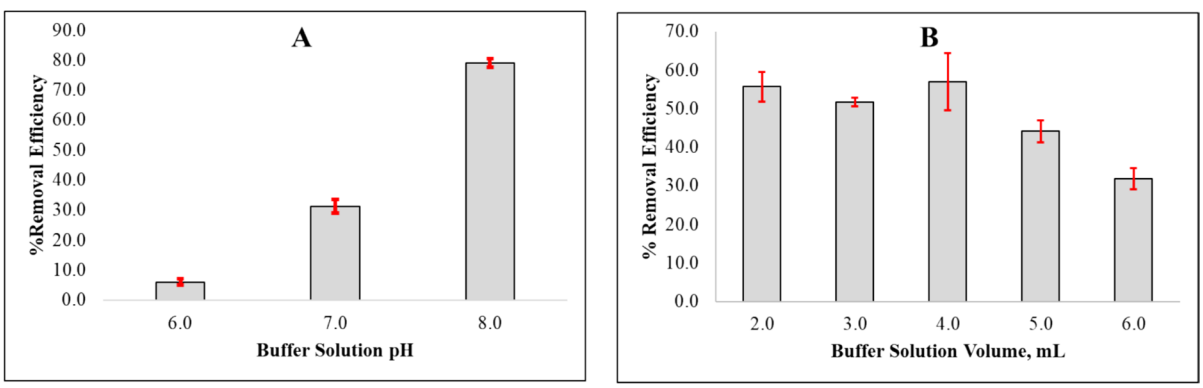

Fig. 5 Effect of pH (**a**) and buffer solution volume (**b**) on extraction efficiency ($n = 3$) (experimental condition for pH: 30 mL standard solution (1.0 mg/L), 4.0 mL buffer solution, 20 mg sorbent, orbital shaking for 15 min. Experimental condition for buffer solution volume: 30 mL standard solution (1.0 mg/L), pH 8.0 buffer solution, 20 mg sorbent, orbital shaking for 15 min)

to decrease significantly due to increased competition between hydrogen ions and metal ions [41]. The solubility of Cd ions is pH-dependent. Cd(II) and $Cd(OH)^+$ species become highly soluble when the pH decreases, resulting in poor adsorbate-adsorbent interactions. Conversely, Cd ions precipitate as metal hydroxides, such as $Cd(OH)_2$, when the pH exceeds 8.0 [3]. Moreover, the alkaline solution medium assists in the precipitation of heavy metal species and this may also be responsible for the increased removal efficiency when the pH of the sample is higher than 8.0 [42]. The highest removal efficiency was recorded at pH 8.0 value. Therefore, the initial sample pH was fixed at 8.0 using a borax-buffer solution.

The effect of buffer solution volume on cadmium extraction was evaluated between 2.0 and 6.0 mL (Fig. 5b). The highest output was obtained with 4.0 mL of buffer solution, while the repeatability of the results decreased. Therefore, 2.0 mL of buffer solution at pH 8.0 was selected as the optimal condition, which provided high efficiency to prevent dilution of analyte ions in the final phase.

Mixing conditions

Various mixing modes, including orbital shaking, vortexing, and ultrasonication, were tested at a constant period of 60 s under similar experimental conditions. Experiments were also performed simultaneously without a mixing process. The optimization of mixing demonstrated that ultrasonication was the most effective mixing method for Cd extraction due to a more efficient distribution of sorbent and improved mass transfer of analytes (Fig. 6a). Moreover, ultrasound is commonly employed in many application fields, especially adsorption and desorption processes of metal ions and organic pollutants, due to its low cost and the necessity of easy [35]. Accordingly, the effect of the ultrasonication period on Cd extraction was investigated in the range of 30–300 s. A fluctuating trend was observed for the Cd extraction during the investigated ultrasonication period (Fig. 6b). This is probably due to the competition between adsorption and desorption processes as the ultrasonication time extends. The optimization study revealed that a 30 s ultrasonication period provided optimum conditions, while extended periods showed decreasing-increasing returns due to the competing adsorption-desorption equilibrium. Hence, a 30 s ultrasonication period was determined as the optimum mixing condition for further studies, as it provided effective dispersion of sorbent in sample medium and enabled maximum extraction efficiency in a short time.

Effect of the CuSn(OH)6 nanoparticles amount

The effect of adsorbent amount was investigated in the range of 0.0 to 50 mg to improve the adsorption performance and minimize the adsorbent usage. The results in Fig. 7a show that the absorbance values gradually increased with increasing amounts and reached a peak at 50 mg. This trend can be explained

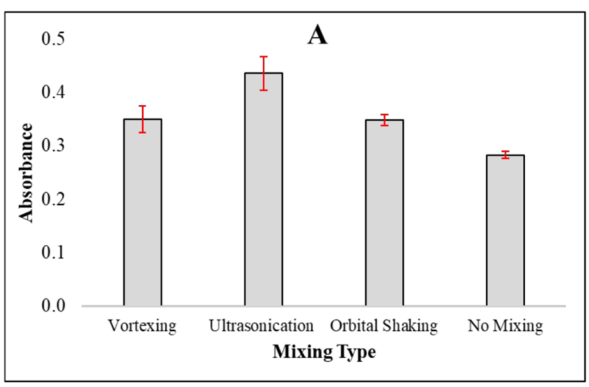

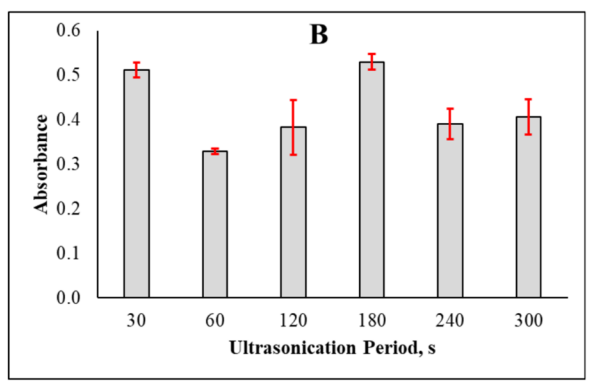

Fig. 6 Effect of mixing type (**a**) and ultrasonication period (**b**) on extraction efficiency ($n = 3$) (experimental condition for mixing type: 30 mL standard solution (0.05 mg/L), 2.0 mL of pH 8.0 buffer solution, 50 mg sorbent, mixing for 60 s, 200 µL of conc. HNO_3. Experimental condition for ultrasonication period: 30 mL standard solution (0.05 mg/L), 2.0 mL of pH 8.0 buffer solution, 40 mg sorbent, ultrasonication mixing, 200 µL of conc. HNO_3)

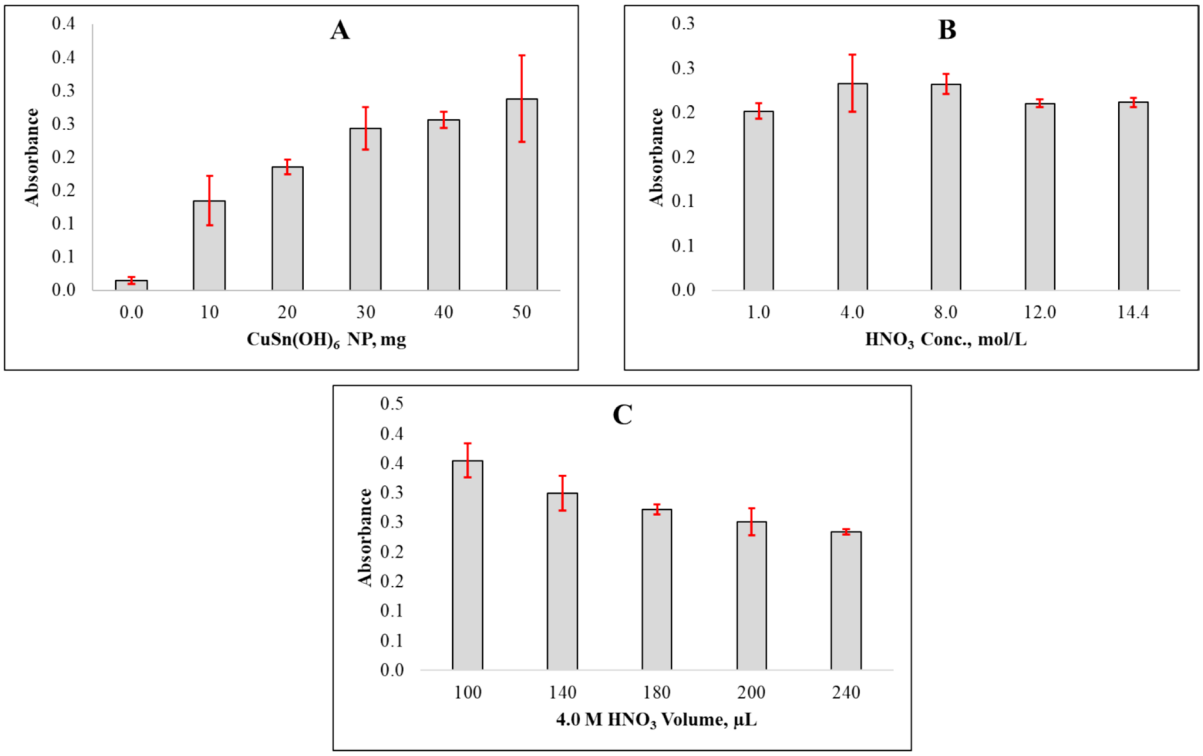

Fig. 7 Effect of sorbent amount (**a**), desorption solution concentration (**b**), and desorption solution volume (**c**) on extraction efficiency ($n=3$) (experimental condition for sorbent amount: 30 mL standard solution (0.05 mg/L), 2.0 mL of pH 8.0 buffer solution, $CuSn(OH)_6$ nanoparticles, ultrasonication for 60 s, 200 µL of conc. HNO_3. Experimental Condition for desorption solution concentration: 30 mL standard solution (0.01 mg/L), 2.0 mL pH 8.0 buffer solution, 40 mg sorbent, ultrasonication for 30 s, 200 µL of desorption solution. Experimental condition for desorption solution volume: 30 mL standard solution (0.01 mg/L), 2.0 mL of pH 8.0 buffer solution, 40 mg sorbent, ultrasonication for 30 s, 4.0 M HNO_3)

by the increase in the number of active sites on the adsorbent surface with increasing amounts. Additionally, there is no detectable analytical signal observed at 0.0 mg, confirming that the extraction process was entirely dependent on the presence of the synthesized material. However, the use of 50 mg adsorbent resulted in low repeatability due to aggregation or the requirement of more desorption solution. Accordingly, the lowest %RSD (< 5.0%) was obtained with 40 mg, which showed high adsorption capacity. Therefore, 40 mg of $CuSn(OH)_6$ nanoparticles was used in the remainder of the studies.

Desorption conditions

In this study, HNO_3 solution was selected as the proper desorption solution due to compatibility with the FAAS system and providing good solubility of analyte ions [15]. The different HNO_3 solution concentrations were studied in the 1.0–14.4 M range to determine the optimal conditions for the release of analyte ions, given in Fig. 7b. The sufficient extraction efficiency was recorded with a 4.0 M HNO_3 solution. Following this, the desorption solution volume was then optimized in the range of 100–240 µL. According to Fig. 7c, the result was linearly decreased with increasing acidic solution volume. This trend can be linked to the dilution of analyte ions in the resulting phase. The highest desorption efficiency was observed at 100 µL; however, this caused a significant challenge during the phase separation process. Hence, 180 µL of 4.0 M HNO_3 solution was determined for the optimal desorption conditions that contribute to minimizing the consumption of mineral acid solution and providing the highest extraction outputs.

Analytical figure of merits

The analytical performance of the $CuSn(OH)_6$ nanoparticles-assisted preconcentration method was examined under the optimized conditions, presented in Table 1. In this study, the blank correction strategy was applied, which involved subtracting the method blank response from each calibration solution. This correction eliminates background contributions from sorbent or sample matrices and overestimated concentrations or deviated calibration curves. The corrected calibration graph exhibits a more accurate calculation for the studied analytes. The regression equation of the FAAS system and the developed method was obtained as $y=0.1454x+0.0045$ (based on mg/L, $R^2=0.9989$) for the FAAS system and $y=0.0114x+0.0075$ (based on µg/L, $R^2=0.9949$) for the corrected calibration graph of the developed method, respectively. The limit of detection (calculated based on $3 \times SD/m$, where SD is the standard deviation of the lowest concentration and m is the slope of the regression equation) and limit of quantification (based on $10 \times SD/m$) were found to be 0.84 and 2.80 µg/L, respectively. The linear calibration plot was in the concentration range of 2.5–50 µg/L for Cd ions. The %RSD, expressed as precision of the presented method, was determined to be 8.9% for the lowest concentration of the FAAS system (0.1 mg/L, $n=6$) and 13.2% for the lowest concentration of the developed method (2.5 µg/L, $n=6$). The performance of the method can be assessed through calibration sensitivity, which is determined by the ratio of calibration slopes between the FAAS system and the preconcentration method. The enhancement in calibration sensitivity (ECS) was calculated via the formula given in Eq. 1. ECS was calculated as 78.6-folds, and comprehensive results are summarized in Table 2.

$$ECS = \frac{Slope\ of\ the\ method\ calibration\ obtained\ from\ FAAS\ for\ Cd}{Slope\ of\ the\ calibration\ without\ method\ obtained\ from\ FAAS\ for\ Cd} \quad (1)$$

Table 2 Comparison of the method presented with other reported techniques

Adsorbent/detection system	LOD[a]	LOQ[b]	Dynamic range	EDP/ECS/PF[c]	REF
FAAS[d]	**0.03 mg/L**	**0.11 mg/L**	**0.1–4.0 mg/L**	**-**	**This study**
$CuSn(OH)_6$ NP/FAAS	**0.84 µg/L**	**2.80 µg/L**	**2.5–50 µg/L**	**78.6**	**This study**
MWCNT@$TiSiO_4$ nanocomposite/FAAS[e]	**0.053 µg/L**	**0.176 µg/L**	**-**	**40**	[38]
MWCNT-Fe_3O_4@SiO_2-SH composite/FAAS[f]	**0.090 µg/L**	**0.302 µg/L**	**0.001–40 µg/L**	**33.14**	[12]
Fe_3O_4@MoS_4^{2-}—FeMgAl LDH nanocomposite/ICP-OES[g]	**0.031 µg/L**	**0.10 µg/L**	**0.1–800 µg/L**	**-**	[18]
ZnO@Fe_3O_4/FAAS	**7.86 µg/L**	**16.9 µg/L**	**50–5000 µg/L**	**-**	[20]
Fe_3O_4@HNT/ICP-OES[h]	**0.037 µg/L**	**0.12 µg/L**	**0.1–400 µg/L**	**73**	[25]
Fe_3O_4@TEOS NP/FAAS[i]	**4.60 µg/L**	**20.0 µg/L**	**20–100 µg/L**	**1.54**	[9]
Fe_3O_4-SiO_2-MIL-53 (Fe) nanocomposite/HR-CS-FAAS[j]	**1.30 µg/L**	**4.3 µg/L**	**4.3–500 µg/L**	**4.9**	[39]

[a] *LOD*, limit of detection

[b] *LOQ*, limit of quantitation

[c] *EDP/ECS/PF*, enhancement in detection power/Enhancement in calibration sensitivity/Preconcentration factor

[d] *FAAS*, flame atomic absorption spectrometry

[e] *MWCNT@TiSiO4*, multi-walled carbon nanotubes@$TiSiO_4$ nanocomposite

[f] *MWCNT-Fe3O4@SiO2-SH*, multiwalled carbon nanotubes decorated with magnetic core–shell Fe_3O_4@SiO_2 and functionalized with 3-mercaptopropyltrimethoxysilane

[g] *Fe3O4@MoS4 2−-FeMgAl LDH nanocomposite/ICP-OES*, MoS_4^{2-}-intercalated magnetic FeMgAl-layered double hydroxide nanocomposite/inductively coupled plasma optical emission spectrometry

[h] *Fe3O4@HNT*, magnetic halloysite nano clay

[i] *Fe3O4@TEOS*, tetraethyl orthosilicate functionalized magnetic iron oxide nanoparticles

[j] *Fe3O4-SiO2-MIL-53 (Fe) nanocomposite/HR-CS-FAAS*, magnetic silica-coated iron oxide—Materials of Institute Lavoisier-53 (Iron) Metal–Organic Framework nanocomposite/high-resolution continuum source flame atomic absorption spectrometry

A comparison between the presented method and other methods reported in the literature for the determination of Cd is listed in Table 2. Nanomaterials were commonly employed for sample preparation techniques. In this study, $CuSn(OH)_6$ nanomaterials were synthesized in only 1.0 h with a simple one-pot coprecipitation method at ambient temperature. Compared to other synthesis techniques, it does not require long analysis periods and high energy consumption. Additionally, $CuSn(OH)_6$ nanoparticles provided a high enrichment factor with lower detection limits for the determination of Cd ions with low amounts and extraction time (just 40 mg and 30 s) in relatively inexpensive instrumentation.

Recovery studies

The analysis of Cd ions in red onion samples was used to validate the applicability and reliability of the method. The aqueous extracts of the samples were prepared according to the "Sampling and preparation of extracts" section, and the method was applied under the optimized experimental conditions. The external calibration strategy and matrix-matching calibration strategy were employed to determine percent recoveries. Firstly, the aqueous extracted red onion samples were tested to determine the presence of the analyte ions. Analytical signals were observed, which are most likely attributed to the characteristics of the nanomaterial or reagents within the detection system. Therefore, signals were corrected according to the mean absorbance value of the blank solution, proving more accurate analysis. The extracted samples had a spiked concentration range between 7.5 and 20 µg/L. An external calibration strategy was applied to ensure accurate quantification of Cd ions. This method involved the comparison between extraction results of aqueous standards and extracted samples, revealing significant insights into the method performance and matrix effects. Moreover, the method applicability was investigated using matrix-matched samples. The matrix-matched calibration regression equation of corrected RO-1 samples ($y = 0.0121x - 0.0149$ based on µg/L) was used to calculate the %recoveries of RO-2 samples. Conversely, the regression equation of RO-2 ($y = 0.0109x + 0.0267$ based on µg/L) was used for the calculation of RO-1 samples. The %recoveries were calculated using Eq. (2).

$$\%Rec = \frac{C_{cal}}{C_{spiked}} \times 100 \quad (2)$$

where C_{Cal} represents the calculated concentration using regression equations of samples and C_{Spiked} represents the initial concentration of the spiked samples.

The obtained results are summarized in Table 3 as mean ± *SD*. These results demonstrate the superior extraction performance and high effectiveness of $CuSn(OH)_6$ for removing cadmium ions from aqueous extracts. The matrix-matching calibration strategy showed significant differences compared to external calibration, with RO-1 exhibiting enhanced recovery (67.2%–96.2%) while RO-2 demonstrated suppressed analytical results (102.1%–131.4%). These contrasting results indicate that matrix effects are sample-dependent. This may be attributable to the

Table 3 The %recoveries for Cd ions determination obtained from red onion extracts using the $CuSn(OH)_6$ nanoparticles

	Spiked concentration, µg/L	External calibration strategy	Matrix-matching calibration strategy
		% Recovery ± *SD*	% Recovery ± *SD*
RO-1	**7.5**	**93.8 ± 7.6**	**74.6 ± 8.0**
	10	**81.1 ± 8.4**	**67.2 ± 8.8**
	12.5	**87.4 ± 2.5**	**77.3 ± 2.6**
	15	**87.6 ± 5.0**	**79.9 ± 5.3**
	20	**100.4 ± 1.3**	**96.2 ± 1.4**
RO-2	**7.5**	**113.3 ± 3.1**	**131.4 ± 2.9**
	10	**117.8 ± 10.5**	**129.5 ± 9.9**
	12.5	**107.5 ± 5.3**	**116.1 ± 5.0**
	15	**95.2 ± 5.8**	**102.1 ± 5.5**
	20	**103.6 ± 5.4**	**106.8 ± 5.1**

[a] *SD*, standard deviation of triplicate measurements

compositional differences between onion samples. The acceptable % recoveries were obtained with the external calibration strategy for both onion samples (81.1%–117.5%), indicating minimal matrix interference effects. Therefore, the presented method can be used as a feasible method for Cd determination/monitoring in plant-derived samples.

Conclusion

This study introduces a $CuSn(OH)_6$ nanoparticle-assisted preconcentration method for the separation/extraction of Cd ions in a plant-derived matrix over a wide linear range. $CuSn(OH)_6$ nanoparticles with uniform morphology were successfully synthesized using a simple one-pot co-precipitation method. Detection and quantification limits were found to be 0.84 µg/L and 2.80 µg/L, respectively, within a wide working range (2.5–50 µg/L). The presented method resulted in remarkable sensitivity enhancement of the FAAS system, improving cadmium detection by approximately 78.6-fold. %recoveries were calculated in the range of 81.1%–117.5% using an external calibration strategy in red onion samples. Considering the widespread consumption of onion worldwide, it is crucial to determine Cd content to ensure the safety and quality of these food products and monitor safe levels for human health and environmental assessment. Accordingly, the method developed using $CuSn(OH)_6$ nanoparticles for the Cd ions showed excellent extraction performance for plant-derived matrixes. These results suggest that the method has potential for facile and straightforward extraction of Cd ions from different plant-derived matrixes.

Acknowledgements We would like to thank the Scientific and Technological Research Council of Turkey (TÜBİTAK) for support through the BİDEB 2211-E National PhD Scholarship Program to M. ŞAYLAN.

Author contribution Meltem Şaylan: Data curation, Formal analysis, Funding acquisition, Methodology, Validation, Writing – original draft Selim Gürsoy: Data curation, Formal analysis, Methodology, Validation, Writing – original draft. Ümmügülsüm Polat Korkunç: Data curation, Formal analysis, Validation, Visualization, Writing – original draft. Buse Tuğba Zaman: Data curation, Formal analysis, Validation, Visualization, Writing – original draft. Sezgin Bakırdere: Conceptualization, Data curation, Funding acquisition, Investigation, Methodology, Supervision, Writing – review & editing.

Funding Open access funding provided by the Scientific and Technological Research Council of Türkiye (TÜBİTAK).

Data availability No datasets were generated or analysed during the current study.

Declarations

Conflict of interest The authors declare no competing interests.

References

1. Abebe Z, Mohammed S, Ejigu A, Lijalem T, Guadie A, Mulu M, Beshaw T, Wubet W, Masresha G, Tefera M (2024) Ecological distribution, heavy metals profiling and human health risk assessment of medicinal plants used for tonsillitis and wounds treatment: a chemometric approach. Environ Adv 15:100503. https://doi.org/10.1016/j.envadv.2024.100503
2. Abu-Darwish MS, Mohammad MY, Abu-Darwish D, Efferth T, Abu-Dieyeh ZH (2024) Heavy metal contents in water extracts of selected medicinal plants used in the folk medicine of Jordan. Phytomedicine Plus 4(4):100634. https://doi.org/10.1016/j.phyplu.2024.100634
3. Aldaghri O, Modwi A, Idriss H, Ali MKM, Ibnaouf KH (2022) Cleanup of Cd II from water media using Y2O3@gC3N4 (YGCN) nanocomposite. Diamond Relat Mater 129:109315. https://doi.org/10.1016/j.diamond.2022.109315
4. Arain MB, Niaz A, Soylak M (2025) Dispersive solid-phase microextraction of Cd(II) using CaFe layer double hydroxide with g-C_3N_4 nanocomposite from food and environmental samples. Food Chem 476:143410. https://doi.org/10.1016/j.foodchem.2025.143410
5. Bibi N, Shah MH, Khan N, Mahmood Q, Aldosari AA, Abbasi AM (2021) Analysis and health risk assessment of heavy metals in some onion varieties. Arab J Chem 14(10):103364. https://doi.org/10.1016/j.arabjc.2021.103364
6. Čeryová N, Judita L, Marek Š, Ľuboš H, Eduard P, Marek B, Alica B, Janette M, Vollmannová A (2024) Heavy metals in onion (*Allium cepa* L.) and environmental and

health risks. Food Addit Contam B 17(1):66–76. https://doi.org/10.1080/19393210.2023.2291369
7. Czarnek K, Tatarczak-Michalewska M, Szopa A, Klimek-Szczykutowicz M, Jafernik K, Majerek D, Blicharska E (2024) Bioaccumulation capacity of onion (Allium cepa L.) tested with heavy metals in biofortification. Molecules 29(1). https://doi.org/10.3390/molecules29010101
8. Dadfarnia S, Haji Shabani AM, Kamranzadeh E (2009) Separation/preconcentration and determination of cadmium ions by solidification of floating organic drop microextraction and FI-AAS. Talanta 79(4):1061–1065. https://doi.org/10.1016/j.talanta.2009.02.004
9. de Souza SA, dos Reis Feliciano C, de Lima GC, da Silva Gomes ÍA, Costa NC, Rocha BA, Santos MG (2025) Rapid and efficient magnetic nanoparticle-based method for Cd determination in Brazilian cachaça using flame atomic absorption spectrometry. Analytica 6(3):33. https://doi.org/10.3390/ANALYTICA6030033/S1
10. Devamani RHP, Alagar M (2013) Synthesis and characterisation of copper II hydroxide nano particles. Nano Biomed Eng 5(3):116–120
11. Dong S, Cui L, Zhao Y, Wu Y, Xia L, Su X, Zhang C, Wang D, Guo W, Sun J (2019) Crystal structure and photocatalytic properties of perovskite MSn(OH)6 (M = Cu and Zn) composites with d10-d10 configuration. Appl Surf Sci 463:659–667. https://doi.org/10.1016/j.apsusc.2018.09.006
12. dos Santos Morales P, dos Mantovani Santos P, de Evaristo Carvalho A, Zanetti Corazza M (2022) Vortex-assisted magnetic solid-phase extraction of cadmium in food, medicinal herb, and water samples using silica-coated thiol-functionalized magnetic multiwalled carbon nanotubes as adsorbent. Food Chem 368:130823. https://doi.org/10.1016/j.foodchem.2021.130823
13. Ebrahimi-Mamaghani M, Saghafi-Asl M, Pirouzpanah S, Asghari-Jafarabadi M (2014) Effects of raw red onion consumption on metabolic features in overweight or obese women with polycystic ovary syndrome: a randomized controlled clinical trial. J Obstet Gynaecol Res 40(4):1067–1076. https://doi.org/10.1111/jog.12311
14. Jaganmohanrao L (2025) Valorization of onion wastes and by-products using deep eutectic solvents as alternate green technology solvents for isolation of bioactive phytochemicals. Food Res Int 206:115980. https://doi.org/10.1016/j.foodres.2025.115980
15. Khalesi S, Fahimirad B, Rajabi M, Baigenzhenov O, Hosseini-Bandegharaei A (2023) Synthesis and comparison of two different morphologies of graphitic carbon nitride as adsorbent for preconcentration of heavy metal ions by effervescent salt-assisted dispersive micro solid phase extraction method. J Dispers Sci Technol 44(11):2093–2102. https://doi.org/10.1080/01932691.2022.2059507
16. Khalili S, Saeidi Asl MR, Khavarpour M, Vahdat SM, Mohammadi M (2022) Comparative study on the effect of extraction solvent on total phenol, flavonoid content, antioxidant and antimicrobial properties of red onion (*Allium cepa*). J Food Meas Charact 16(5):3578–3588. https://doi.org/10.1007/s11694-022-01446-7
17. Khan RRM, Saleem R, Bashir R, Pervaiz M, Naz S, Rehman SU, Younas U, Batool S, Haider HMF, Iqbal M, Adnan A (2021) Highly selective and efficient porous Cu-Sn bimetallic electrocatalyst for CO_2 reduction to formate. Pol J Environ Stud 30(5):4579–4585. https://doi.org/10.15244/pjoes/130975
18. Khunou BP, Nomngongo PN, Nyaba L (2024) Application of MoS42−intercalated magnetic layered double hydroxide for preconcentration of cadmium and lead from water samples. J Hazard Mater Adv 15:100446. https://doi.org/10.1016/j.hazadv.2024.100446
19. Kim K-A, Yim J-E (2015) Antioxidative activity of onion peel extract in obese women: a randomized, double-blind, placebo controlled study. J Cancer Prev 20(3):202
20. Korkmaz Ş, Hasanoğlu Özkan E, Uzun D, Kurnaz Yetim N, Özcan C (2025) Magnetic solid phase extraction of lead (II) and cadmium (II) from water samples using ZnO@Fe3O4 nanoparticles combined with flame atomic absorption spectrometry determination. J Sep Sci 48(3):e70115
21. Li J, Lee SH, Lee JE, Park H-M, Choi B, Choi J-S, Lee HJ (2023) Highly sensitive voltammetric sensor comprising CuSn(OH)6–multi-walled carbon nanotubes–β-cyclodextrin composites and poly(L-arginine) for indole-3-lactic acid analyses in alcohol use disorder serum samples. Electrochim Acta 471:143387. https://doi.org/10.1016/j.electacta.2023.143387
22. Li Y, Rahman SU, Qiu Z, Shahzad SM, Nawaz MF, Huang J, Naveed S, Li L, Wang X, Cheng H (2023) Toxic effects of cadmium on the physiological and biochemical attributes of plants, and phytoremediation strategies: a review. Environ Pollut 325:121433. https://doi.org/10.1016/j.envpol.2023.121433
23. Li Z, Zhang M, Yang L, Wu R, Wu Z, Jiang Y, Zhou L, Liu Y (2022) The effect of surface hydroxyls on the humidity-sensitive properties of LiCl-doped ZnSn(OH)6 sphere-based sensors. Nanomaterials 12(3):467. https://doi.org/10.3390/NANO12030467
24. Liu X, Hao Y, Shu J, Sari HMK, Lin L, Kou H, Li J, Liu W, Yan B, Li D, Zhang J, Li X (2019) Nitrogen/sulfur dual-doping of reduced graphene oxide harvesting hollow ZnSnS3 nano-microcubes with superior sodium storage. Nano Energy 57:414–423. https://doi.org/10.1016/j.nanoen.2018.12.024
25. Mabaso NB, Mnguni M, Nomngongo PN, Nyaba L (2025) Ultrasonic-aided dispersive solid-phase microextraction employing magnetic halloysite nano clay for simultaneous preconcentration of lead (II) and cadmium (II). Green Anal Chem 12:100219. https://doi.org/10.1016/j.greeac.2025.100219
26. Mallamaci R, Conforti F, Statti G, Avato P, Barbarossa A, Meleleo D (2024) Phenolic compounds from Tropea red onion as dietary agents for protection against heavy metals toxicity. Life. https://doi.org/10.3390/life14040495
27. Mirzazadeh N, Bagheri H, Mirzazadeh M, Soleimani-mehr S, Rasi F, Akhavan-Mahdavi S (2024) Comparison of different green extraction methods used for the extraction of anthocyanin from red onion skin. Food Sci Nutr 12(10):7347–7357. https://doi.org/10.1002/fsn3.4354
28. Muni Babu B, Sivakumar R, Sanjeeviraja C (2022) Studies on the properties of copper tin hydroxide-based catalysts prepared by co-precipitation method for photocatalytic degradation of methylene blue dye. J Mater Sci Mater Electron 33(15):11687–11700. https://doi.org/10.1007/s10854-022-08135-7

29. Orzoł A, Gołębiowski A, Szultka-Młyńska M, Głowacka K, Pomastowski P, Buszewski B (2022) ICP-MS analysis of cadmium bioaccumulation and its effect on pea plants (*Pisum sativum* L.). Pol J Environ Stud 31(5):1–9
30. Qin J, Su Z, Mao Y, Liu C, Qi B, Fang G, Wang S (2021) Carboxyl-functionalized hollow polymer microspheres for detection of trace metal elements in complex food matrixes by ICP-MS assisted with solid-phase extraction. Ecotoxicol Environ Saf 208:111729. https://doi.org/10.1016/j.ecoenv.2020.111729
31. Rao Pasupuleti R, Ku Y-J, Tsai T-Y, Hua H-T, Lin Y-C, Shiea J, Huang P-C, Andaluri G, Ponnusamy VK (2023) Novel fast pesticides extraction (FaPEx) strategy coupled with UHPLC-MS/MS for rapid monitoring of emerging pollutant fipronil and its metabolite in food and environmental samples. Environ Res 217:114823. https://doi.org/10.1016/j.envres.2022.114823
32. Reyes-Garcés N, Gionfriddo E, Gómez-Ríos GA, Alam MN, Boyacl E, Bojko B, Singh V, Grandy J, Pawliszyn J (2018) Advances in solid phase microextraction and perspective on future directions. Anal Chem 90(1):302–360
33. Samsonenko M, Zakutevskyy O, Khalameida S, Charmas B, Skubiszewska-Zięba J (2019) Influence of mechanochemical and microwave modification on ion-exchange properties of tin dioxide with respect to uranyl ions. Adsorption 25(3):451–457. https://doi.org/10.1007/s10450-019-00036-2
34. Sangili A, Vinothkumar V, Chen S-M, Veerakumar P, Chang C-W, Panneer Muthuselvam I, Lin K-C (2020) Highly selective voltammetric sensor for l-tryptophan using composite-modified electrode composed of CuSn(OH)6 microsphere decorated on reduced graphene oxide. J Phys Chem C 124(47):25821–25834. https://doi.org/10.1021/acs.jpcc.0c07197
35. Shen D, Labreche F, Wu C, Fan G, Li T, Dou J, Zhu J (2022) Ultrasound-assisted adsorption/desorption of jujube peel flavonoids using macroporous resins. Food Chem 368:130800
36. Shishov A, Gerasimov A, Bulatov A (2022) Deep eutectic solvents based on carboxylic acids for metals separation from plant samples: elemental analysis by ICP-OES. Food Chem 366:130634. https://doi.org/10.1016/j.foodchem.2021.130634
37. Shyam Sunder GS, Adhikari S, Rohanifar A, Poudel A, Kirchhoff JR (2020) Evolution of environmentally friendly strategies for metal extraction. Separations 7(1):4. https://doi.org/10.3390/SEPARATIONS7010004
38. Soylak M, Mohammed AMA, Ahmed HEH (2024) MWCNT@TiSiO4 nanocomposite for dispersive solid phase extraction of traces cadmium in food and environmental samples. J Food Compos Anal 130:106167. https://doi.org/10.1016/j.jfca.2024.106167
39. Soylak M, Uzcan F, Goktas O, Gumus ZP (2023) Fe3O4-SiO2-MIL-53 (Fe) nanocomposite for magnetic dispersive micro-solid phase extraction of cadmium (II) at trace levels prior to HR-CS-FAAS detection. Food Chem 429:136855. https://doi.org/10.1016/J.FOODCHEM.2023.136855
40. Stasinos S, Zabetakis I (2013) The uptake of nickel and chromium from irrigation water by potatoes, carrots and onions. Ecotoxicol Environ Saf 91:122–128. https://doi.org/10.1016/j.ecoenv.2013.01.023
41. Tokalıoğlu Ş, Shahir S, Yılmaz Y, Patat Ş (2024) Selective and fast magnetic dispersive solid phase micro-extraction of copper and lead in water and vegetables after synthesis of magnetic mesoporous carbon. Talanta 266:125002. https://doi.org/10.1016/j.talanta.2023.125002
42. Wu J, Wang T, Wang J, Zhang Y, Pan W-P (2021) A novel modified method for the efficient removal of Pb and Cd from wastewater by biochar: enhanced the ion exchange and precipitation capacity. Sci Total Environ 754:142150. https://doi.org/10.1016/j.scitotenv.2020.142150
43. Yilmaz E, Soylak M (2016) Latest trends, green aspects, and innovations in liquid-phase–based microextraction techniques: a review. Turk J Chem 40(6):868–893. https://doi.org/10.3906/kim-1605-26
44. Zhou Z, Chen T, Deng J, Yao Q, Wang Z, Zhou H (2018) CuSn(OH)6 nanocubes as high-performance anode materials for lithium-ion batteries. Int J Electrochem Sci 13(2):2001–2009. https://doi.org/10.20964/2018.02.72